doi:10.1017/S1431927621004487
Microsc. Microanal. 27 (Suppl 1), 2021
© Microscopy Society of America 2021

Space- and Angle-Resolved Vibrational Spectroscopy to Probe the Local Phonon Modes at Planar Defects

Xingxu Yan[1], Chaitanya Gadre[2], Toshihiro Aoki[3], Tracy Lovejoy[4], Niklas Dellby[4], Ondrej Krivanek[4] and Xiaoqing Pan[2]

[1]Department of Materials Science and Engineering, University of California - Irvine, Irvine, California, United States, [2]Department of Physics and Astronomy, University of California, Irvine, CA 92697, Irvine, California, United States, [3]Irvine Materials Research Institute, University of California, Irvine, Irvine, California, United States, [4]Nion R&D, 11511 NE 118th St, Kirkland, WA, 98034, USA, United States

Combined with aberration-corrected scanning transmission electron microscopy (STEM) imaging, the state-of-the-art monochromated electron energy-loss spectroscopy (EELS) is capable of detecting vibrational spectra for a variety of materials with an attainable energy resolution less than 10 meV and sub-nanometer resolution [1, 2]. Additionally, by varying the convergence semi-angle (α) and EELS collection geometry, momentum resolution is achieved, enabling angle-resolved vibrational spectroscopy that maps out the phonon dispersion relations [3]. Balancing these three aspects: spatial, energy, and momentum resolutions, we can obtain a powerful space- and angle-resolved vibrational spectroscopy to investigate local phonon modes near the crystalline defects in semiconductors and their heterostructures [4]. Planar defects such as stacking faults and interfaces are believed to impede phonon propagation and modify the vibrational structure [5]. However, the experimental evidence of phonon-defect interactions is fundamentally elusive from either thermal conductivity measurements or optical spectroscopies due to their insufficient spatial resolution. Here we show two cases to demonstrate how to utilize the high spatial, energy, and momentum resolution capabilities of monochromated EELS to reveal the local defect phonon modes at (1) a stacking fault in cubic silicon carbide and (2) an interface in a Si–Ge heterojunction.

Stacking faults are common imperfections in SiC, and remarkably affect the bulk thermal conductivity [6]. To isolate individual phonon branches, we chose $\alpha = 3$ mrad (0.5 Å^{-1} momentum resolution) and collected vibrational signals at the X point on the edge of Brillouin zone. With a spatial resolution of about 2.6 nm in this condition, we can still identify the location of stacking fault, as shown in Fig. 1(a). Fig. 1(b) shows the line-scan angle-resolved vibrational spectra, which contain three discernable peaks corresponding to transverse acoustic (TA), longitudinal acoustic (LA) and a mixture of longitudinal/transverse optical (LO/TO) phonons. At the stacking fault, the acoustic phonons undergo an energy red shift of 3.8 meV and major intensity modulations. These striking features arise from the symmetry breaking and variation of interatomic force constants and are assigned to the local defect phonon modes. Moreover, the spatial distribution of defect phonon modes is revealed from the line profiles of the energy shift (Fig. 1c) and signal intensity (Fig. 1d). Both peak widths (7.8 nm/6.8 nm) are considerably larger than either the structural size of stacking fault (0.25 nm) or the beam broadening (2.6 nm). The increased width can be explained by the penetration of the defect phonon modes into the surrounding SiC region. Both the reduced phonon energy and flattened dispersion curves of defect phonon modes help understand the defect-induced reduction of thermal conductivity [4].

In the second case, we employed a similar strategy to probe the interface mode at a Si-Ge epitaxial interface, which is predicted to facilitate the heat transport across interface [7]. To distinguish the atomically sharped interface, a large convergence semi-angle ($\alpha = 33$ mrad) setting was chosen for vibrational spectroscopy with a spatial resolution of 1.5 Å. Fig. 2b plots the line-scan of vibrational

CrossMark

https://doi.org/10.1017/S1431927621004487 Published online by Cambridge University Press

spectra, showing the optical phonon modes of Si and Ge at 60 meV and 34 meV, respectively. Interestingly, there are extra signals at 48 meV (11.6 THz) near the interface, which is absent in the vibrational structure of either Si or Ge [7]. The line profiles of signal intensity in Fig. 2c demonstrate only the 48-meV signal is localized at the interface and exhibits a Gaussian distribution centered at the interface with a width of 1.3 nm. Furthermore, angle-resolved vibrational spectra also confirm the occurrence of the dispersionless interface modes. The localized interface phonon mode is consistent with first-principles calculation results and thermal conductance measurements. Our work opens the door to investigating phonon propagation around crystal defects and provides guidance to the engineering of desired heat management for semiconductor and power electronic devices [8].

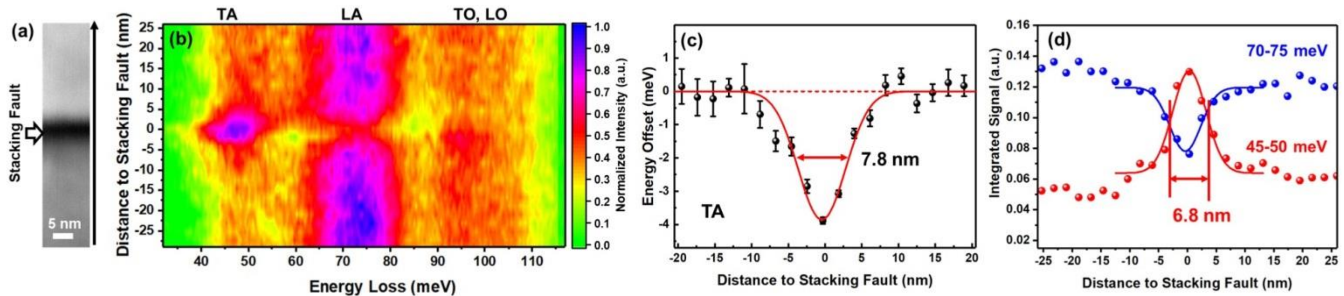

Figure 1. Figure 1. Angle-resolved vibrational spectra of local defect phonon resonance near stacking fault under small convergence semi-angle (α) of 3 mrad. (a) STEM image containing a stacking fault. Scale bar: 5 nm. (b) Line profile of the vibrational spectra at X point along the direction denoted by the black arrow in (a). Color scale shows the signal intensity normalized by its maximum. (c) Energy offset of the 40–50 meV peak in (b) as a function of distance. Peak centers were determined by a peak fitting process, and then subtracted by the energy value of TA mode (49 meV) in defect-free SiC. The red curve is a Gaussian fitting. (d) Integrated signals of TA (red dots) and LA (blue dots) in the respective energy ranges 45–50 meV and 70–75 meV in (b), overlapping with Gaussian fitting curves.

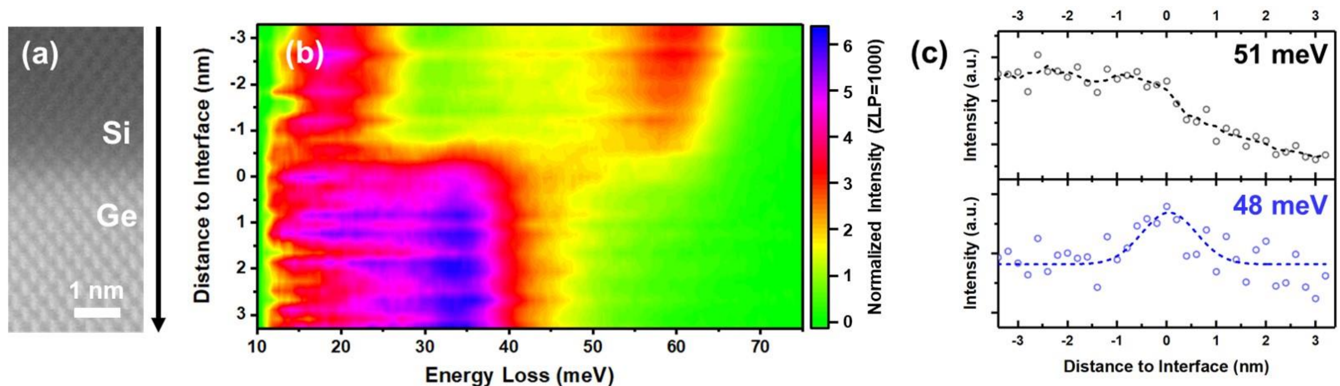

Figure 2. Figure 2. Vibrational spectra across a Si-Ge interface under large convergence semi-angle of 33 mrad. (a) STEM image at the interface through [110] zone axis. Scale bar: 1 nm. (b) Line profile of spatially resolved vibrational spectra along the direction denoted by the black arrow in (a). Color scale shows the intensity normalized by the zero-loss peak height. (c) Line profile of intensity at 51 meV (top) and 48 meV (bottom) in (b), overlapping with a smoothed curve and a Gaussian fitting curve, respectively.

References

[1] O. L. Krivanek *et al.*, Nature **514** (2014), p. 209−212.

https://doi.org/10.1017/S1431927621004487 Published online by Cambridge University Press

[2] K. Venkatraman *et al.*, Nat. Phys. **15** (2019), p. 1237–1241.

[3] R. Senga *et al.*, Nature **573** (2019), p. 247–250.

[4] X. X. Yan *et al.*, Nature **589**, (2021), p. 65–69.

[5] M. D. Li *et al.*, Nano Lett. **17** (2017), p. 1587−1594.

[6] J. S. Goela *et al.*, in High Thermal Conductivity Materials, (Springer, 2006) p. 167–198.

[7] Y. Chalopin and S. Volz, Appl. Phys. Lett. **103** (2013), 051602.

[8] This work was supported by the Department of Energy, Office of Basic Energy Sciences, Division of Materials Sciences and Engineering (DE-SC0014430). The authors acknowledge the use of facilities and instrumentation at the UC Irvine Materials Research Institute (IMRI) supported in part by the National Science Foundation through the Materials Research Science and Engineering Center program (DMR-2011967). TEM experiments were conducted using the Nion UltraSTEM 200 with HERMES operating at 60 keV.

https://doi.org/10.1017/S1431927621004487 Published online by Cambridge University Press